IRJIEST 8 (2022) 26 - 31
Available online at https://ojs.batstate-u.edu.ph
International Research Journal on Innovations in Engineering, Science and Technology

Deep autoencoders for denoising computerized tomography (CT) images

Aunhel John M. Adoptante[a,b], Alvin S. Alon[a,*], Sandhya Avasthi[c]
[a]*Batangas State University, Batangas City, Batangas, Philippines*
[b]*Department of Science and Technology – Advanced Science and Technology Institute, Diliman, Quezon City, Philippines*
[c]*Department of Computer Science and Engineering– ABES Engineering College, Ghaziabad, India*

ABSTRACT

Understanding the complexities of human biology and making accurate medical diagnoses depend heavily on medical imaging technologies. However, a major barrier to proper analysis is the problem of noise interference in imaging. In this study, we use deep autoencoders to solve the common problem of noise reduction in computed tomography (CT) images, specifically in the 100-image Cancer Genome Atlas Lung Adenocarcinoma (TCGA-LUAD) dataset. The study measures the structural similarity index (SSIM) to evaluate the denoising performance of a sequential model using Keras. To improve the model's flexibility in real-world circumstances, Poisson noise has been introduced into the dataset. During training and validation, the model achieved significant accuracy rates of 85.63% and 88.02%, respectively, with an average SSIM score of 0.7613 for the test data. This study sheds light on the significance of deep autoencoders in advancing the domain of medical imaging, particularly in enhancing CT image reconstructions by effectively reducing noise interference while preserving crucial structural details. The findings pave the way for future refinements in deep learning methodologies tailored for medical imaging applications, offering a promising avenue toward improved diagnostic imaging in healthcare.

Keywords: autoencoder, denoising, medical imaging, unsupervised learning, deep autoencoder

1. Introduction

Medical imaging plays a significant role in the diagnosis and treatment of many different medical illnesses [1]. It allows for non-invasive imaging of the internal organs and biological functions, providing doctors and nurses with crucial information. However, the images produced by these methods typically contain noise, which can make it challenging to comprehend and properly evaluate them [2].

Medical imaging noise can originate from several sources, including the imaging modality itself, the subject being imaged, and the environment in which the imaging is performed [3]. These irregular intensity shifts, aberrations, and other distortions caused by the noise could mask important image details and lead to a partial or incorrect diagnosis [4].

Denoising, or the technique of eliminating noise from images, is therefore an essential step in the medical image processing pipeline. Accurate diagnosis and treatment plans can be made possible by medical images that have been cleaned of noise and made clearer and more accurate [5]. Automated diagnostic tools and other applications may be developed more easily since denoised images are also easier for computer algorithms to interpret [6].

For medical image denoising, both conventional image processing methods and machine learning algorithms have been used in the past [7]. For example, noise from medical imaging has been removed using filters based on spatial information and image statistics [8], and noise patterns in images have been identified and removed using support vector machines [9] and k-nearest neighbors [10,11] models.

Autoencoders have recently become recognized as a potential method for denoising medical pictures [12]. Autoencoders are neural networks that can learn to extract significant elements from images and rebuild a denoised version of the image using these features [13]. When compared to conventional denoising techniques, this method has a number of benefits, including the ability to handle complicated and highly variable noise patterns and the capacity to learn from a large number of training instances [14].

Deep autoencoders will be the primary method for denoising medical images, particularly computerized tomography (CT) images, in this study. We will go through the benefits of deep autoencoders and showcase an example that uses actual medical photos to show how effective they are. The study focuses on the strategic use of deep autoencoders for denoising in CT images. Our primary aim is to show that these advanced neural networks can successfully reduce noise from CT scans, increasing the clarity of the image. We hope to improve not just the precision and reliability of medical imaging by using the intrinsic capability of deep autoencoders, but also to give clearer, more accurate diagnostic information that may considerably aid clinical decision-making and patient care.

Recent studies utilizing denoising autoencoders for different medical imaging applications gave a better overview on how to improve various medical procedures and diagnosis. The low number of medical images for contemporary disorders connected to pneumonia makes medical diagnosis

*Corresponding author
Email address: mariellikatherine.untalan@g.batstate-u.edu.ph

of pneumonia a major challenge. While experiments with various models have not yet yielded satisfying results, transfer learning is a potential approach for transferring knowledge from general to specific tasks. [15] recommended using the CADTra automatic detection model, which employs classification, denoising autoencoder, and transfer learning to diagnose pneumonia-related disorders. To maximize the odds of retrieving inputs and enhancing the diagnosis process, preprocessing is used with an autoencoder denoising method with a modified loss function. To identify pneumonia, a transfer learning model and a four-layer convolutional neural network are used for classification. In comparison to current state-of-the-art CNN models, the suggested model is more effective, achieving precisions of 98% and 99% for binary and multiclass classification, respectively.

Important information required for medical diagnosis are typically obscured by noise in speckle-prone optical coherence tomography. A denoising strategy for preserving disease characteristics on retinal optical coherence tomography images in ophthalmology is provided in [16]. During training, the proponents proposed semantic denoising autoencoders that combine a convolutional denoising autoencoder with a previously trained ResNet image classifier as a regularizer. By removing only the background noise that provides no useful information, this enhances the visibility of subtle details in the denoised images that are crucial for diagnosis. When compared to state-of-the-art denoising, this method achieves higher peak signal-to-noise ratios with PSNR = 31.0 dB and higher classification performance with F1 = 0.92 for denoised images. It has been demonstrated that semantically regularized autoencoders may denoise retinal OCT pictures without obscuring disease features.

The electrocardiogram (ECG) is a commonly used instrument for detecting and preventing arrhythmia. In most instances, it produces reliable results and is non-invasive, meaning it doesn't involve making physical contact with the patient. Unfortunately, ECG signals can be affected by many types of noise, which can lead to inaccurate diagnosis or analysis. Researchers of [17] have suggested employing denoising autoencoders (DAEs), which can reconstruct clean data from its noisy equivalent, to solve this problem. In this particular paper, a DAE based on fully convolutional networks (FCN) has been presented for both ECG signal denoising and compression of the input signals down to 32 times their original size. Metrics like root-mean-square error (RMSE), percentage root mean square difference (PRD), and an improvement in signal-to-noise ratio were used to gauge the model's performance (SNRimp). When it comes to denoising noisy ECGs at different levels of input SNR values, the results reveal that FCN outperforms other deep neural network models, showing good application prospects in clinical practice in the future.

In order to improve the image clarity of noisy mammograms, a deep unsupervised learning algorithm for degraded mammography restoration was used in this research. For mammography restoration, a deep convolutional denoising autoencoder method based on total variational multi-norm loss function minimization has been presented in [18]. The proposed approach can preserve the important characteristics that have been used to restore image data in feature space while extracting pertinent features and reducing the dimensionality of the image data. Eventually, unsupervised learning is carried out based on the relationship between important features and the weighted parameters of the network model. Results from experiments confirm that the proposed strategy outperforms a number of state-of-the-art techniques.

2. Materials and methods

2.1. Dataset

Datasets are the foundations for training, analyzing, and evaluating machine learning models, and they have played an important role in the discipline's advancement [19]. In this work, we used a smaller sample of photos from the cancer imaging collection of The Cancer Genome Atlas Lung Adenocarcinoma (TCGA-LUAD) [20] . By providing clinical images matched to subjects from The Cancer Genome Atlas [21], the TCGA-LUAD data collection is a part of a larger initiative to create a research community focused on tying cancer phenotypes to genotypes. The data used in this experiment contain one hundred distinct images of the middle slice of all CT images acquired where correct age, modality, and contrast tags could be discovered. Sample images from the dataset are shown in Figure 1. Each image is in .tiff format, with a size of 512 x 512 pixels. Data is taken from: https://www.kaggle.com/datasets/kmader/siim-medicalimages

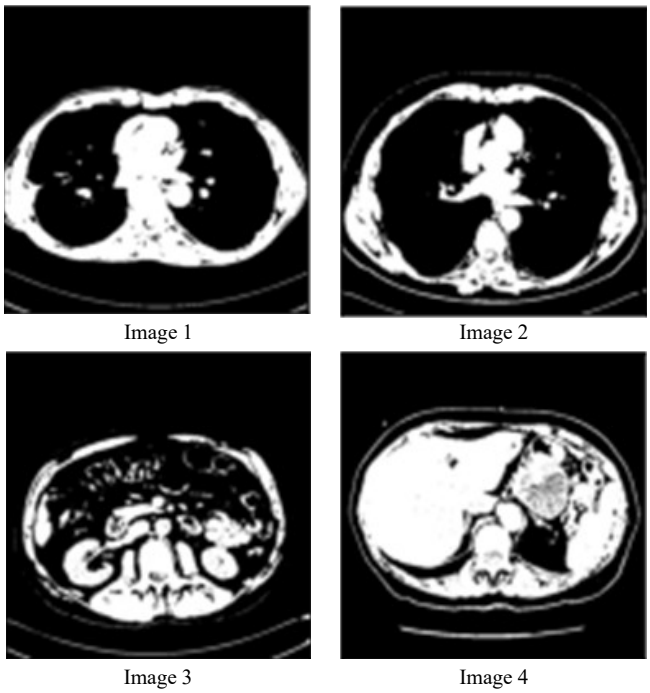

Figure 1. Sample images from dataset.

2.2. Data processing

Preprocessing and data preparation are crucial steps in every machine learning operation. It comprises a series of steps to prepare the data for modeling and analysis.

In this study, the first step was to convert every image in the dataset to a .jpg format. The data was then randomly

divided into training and test sets once the images have been formatted correctly. This is crucial because test data will be used to evaluate the model's performance once it has been trained on training data. Of the total data, 20% was used for testing data and 80% was designated as training data.

The study also presented the idea of "poison noise," which is the purposeful alteration of input data to trick machine learning models. To do this, Poisson noise was applied to the images. Poisson noise is a statistical noise type that is frequently observed in images and is brought on by pixel intensity values fluctuating randomly [22]. By adding this noise to the training and test data, we potentially enhance the model's resilience and more precisely imitate actual scenarios [6]. Mathematically, Poisson noise can be represented as:

$$Noisy\ Data = X + \varepsilon \quad (1)$$

where X represents the original data and ε signifies the noise, which follows a Poisson distribution with a mean parameter λ.

The Poisson distribution's variance, or mean, is represented by the symbol λ. The probability mass function of the Poisson distribution is given by:

$$P(X = k) = \frac{\lambda^k e^{-\lambda}}{k!} \quad (2)$$

Here, k represents the number of events occurring, e is the base of the natural logarithm, λ is the average number of events, and $k!$ denotes the factorial of k.

The Poisson noise is added to the original data, causing a certain degree of perturbation based on the distribution of events as characterized by λ. This perturbation can affect the data in a way that misleads the model during training or inference, emphasizing the need for robust models capable of handling such variations and disturbances.

A Poisson noise with λ = 1.00 was added to the original dataset to create their noisy counterparts. Samples of the original images and their noisy counterparts can be visualized in Figure 2.

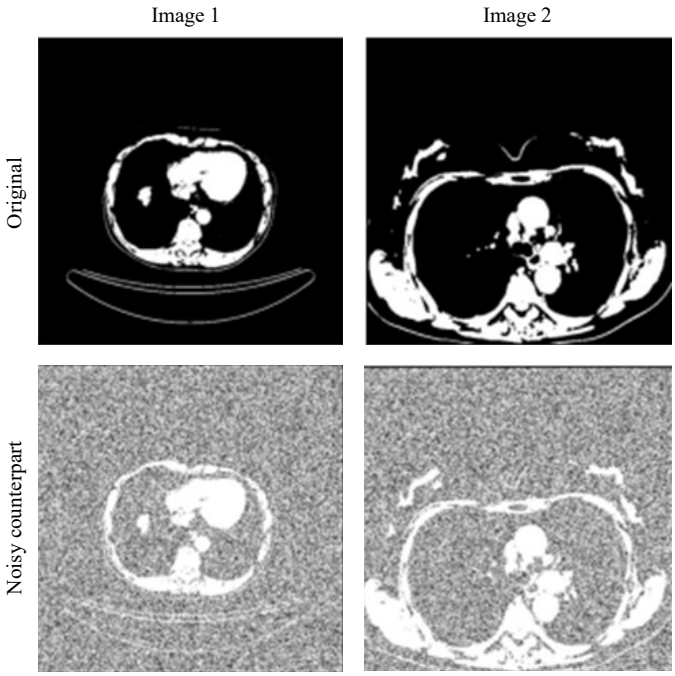

Figure 2. Sample of the original images and their noisy counterparts.

2.3. Autoencoder architecture

The study employed an autoencoder architecture detailed in Table 1, constructed as a Sequential model using the Keras library [23]. This autoencoder consisted of an encoder comprising four layers, each layer housing 128, 64, 32, and 16 nodes, consecutively. ReLU activation functions were employed for each layer in the encoder, facilitating non-linearity and information extraction.

Table 1. Model architecture.

Layer (type)	Output Shape	No. of Parameters
conv2d (Conv2D)	(None, 512, 512, 128)	1280
maxpooling2d	(None, 256, 256, 128)	0
(MaxPooling2D) conv2d$_1$(Conv2D)	(None, 256, 256, 64)	73792
maxpooling2d$_1$	(None, 128, 128, 64)	0
(MaxPooling2D) conv2d$_2$(Conv2D)	(None, 128, 128, 32)	18464
maxpooling2d$_2$	(None, 64, 64, 32)	0
(MaxPooling2D) conv2d$_3$(Conv2D)	(None, 64, 64, 16)	4624
maxpooling2d$_3$	(None, 32, 32, 16)	0
(MaxPooling2D) conv2d$_4$(Conv2D)	(None, 32, 32, 16)	2320
upsampling2d	(None, 64, 64, 16)	0
(UpSampling2D) conv2d$_5$(Conv2D)	(None, 64, 64, 32)	4640
upsampling2d$_1$	(None, 128, 128, 32)	0
(UpSampling2D) conv2d$_6$(Conv2D)	(None, 128, 128, 64)	18496
upsampling2d$_2$	(None, 256, 256, 64)	0
(UpSampling2D) conv2d$_7$(Conv2D)	(None, 256, 256, 128)	73856
upsampling2d$_3$	(None, 512, 512, 128)	0
(UpSampling2D) conv2d$_8$(Conv2D)	(None, 512, 512, 1)	1153

Model: Sequential
Total params: 198,625
Trainable params: 198,625
Non-trainable params: 0

Conversely, the decoder mirrored the structure of the encoder, featuring four layers with node configurations of 16, 32, 64, and 128. Similar to the encoder, ReLU activation functions were utilized across the decoder's layers. The output layer employed a sigmoid activation function, emphasizing the generation of outputs within the [0, 1] range.

The architecture utilized the Adam optimizer, binary cross entropy as the loss function, and accuracy as the metric to compile the model. This configuration aimed to optimize the network's weights and biases during the training process, minimizing the discrepancy between predicted and actual values.

Moreover, the model underwent training for 50 epochs, each consisting of a batch size of 8. This choice of hyperparameters facilitated the iterative learning process, refining the model's ability to reconstruct input data.

2.4. Evaluation metrics

In the evaluation of image denoising, structural similarity index measure (SSIM), as opposed to peak signal to noise ratio (PSNR), is used to compare the results with the original images because it is more reliable and consistent [24]. The SSIM is a comprehensive index, which is made up of three indicators, that determines the impact of structural alterations on vision,

also known as changes in image brightness, contrast, and other lingering defects [25].

Given the original image x and the denoised image y, we can determine the SSIM by

$$SSIM(x,y) = [l(x,y)]^{\alpha}[c(x,y)]^{\beta}[s(x,y)]^{\gamma} \quad (3)$$

where α, β and γ > 0 control the relevance of each of three terms in SSIM and l, c and s are luminance (4), contrast (5) and structural elements (6), which are calculated by

$$l(x,y) = \frac{2\mu_x\mu_y+C_1}{\mu_x^2+\mu_y^2+C_1} \quad (4)$$

$$c(x,y) = \frac{2\sigma_x\sigma_y+C_2}{\sigma_x^2+\sigma_y^2+C_2} \quad (5)$$

$$s(x,y) = \frac{2\sigma_{xy}+C_3}{\sigma_{xy}+C_3} \quad (6)$$

where μx and μy represent the means of the original and coded images, respectively, σx and σy are their respective standard deviations, and σxy is their covariance.

3. Results and discussion

The relatively close values between the Training Loss (0.1278) and Validation Loss (0.1052) suggest a model that effectively learns the features within the CT images while generalizing well to unseen data as shown in Figure 3 and Figure 4. The high values of both Accuracy in Training (0.8563) and Validation (0.8802) further support the model's proficiency in denoising CT images, showcasing a high level of precision in correctly identifying and reconstructing the underlying patterns within the images as shown in Table 2.

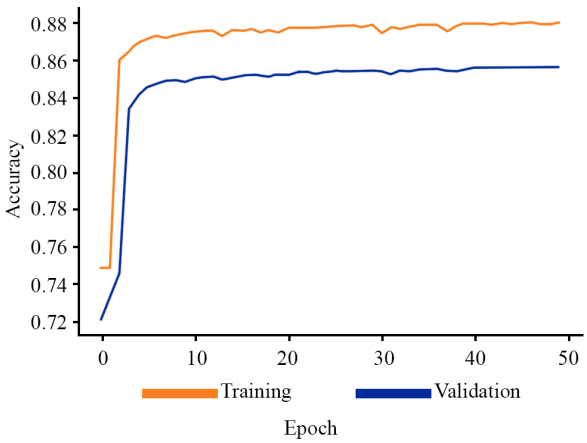

Figure 3. Model accuracy.

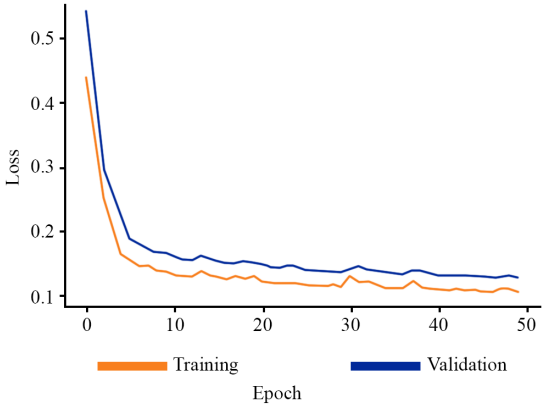

Figure 4. Model loss.

Table 2. Structural Similarity Index Measure (SSIM) between test images and denoised reconstructed images.

Test image number	Reconstructed image number	Structural similarity index measure (SSIM)
1	1	0.5721
2	2	0.8296
3	3	0.7075
4	4	0.7340
5	5	0.7959
6	6	0.8496
7	7	0.6910
8	8	0.7660
9	9	0.7540
10	10	0.7715
11	11	0.7170
12	12	0.8016
13	13	0.7396
14	14	0.8010
15	15	0.7681
16	16	0.7869
17	17	0.8072
18	18	0.7907
19	19	0.7624
20	20	0.7810
	Average	0.7613

Individual SSIM values for each test image and its denoised counterpart indicate how well the deep autoencoder model preserved the essential structural details present in the original CT scans during the denoising process. For instance, test images with higher SSIM values, like image 6 with an SSIM of 0.8496, indicate a strong preservation of structural information in the denoised output. On the other hand, lower SSIM values, such as image 1 with an SSIM of 0.5721, might suggest a relatively lower similarity in structural details between the original and denoised images.

The average SSIM of 0.7613 across all test images demonstrates an overall moderate to good similarity between the original test images and their respective Denoised Reconstructed Images. This suggests that the deep autoencoder model generally performed well in preserving essential structural information during the denoising process. Figure 5 shows the comparison of random images from the test data, its corresponding noisy image, and its denoised reconstructed counterpart.

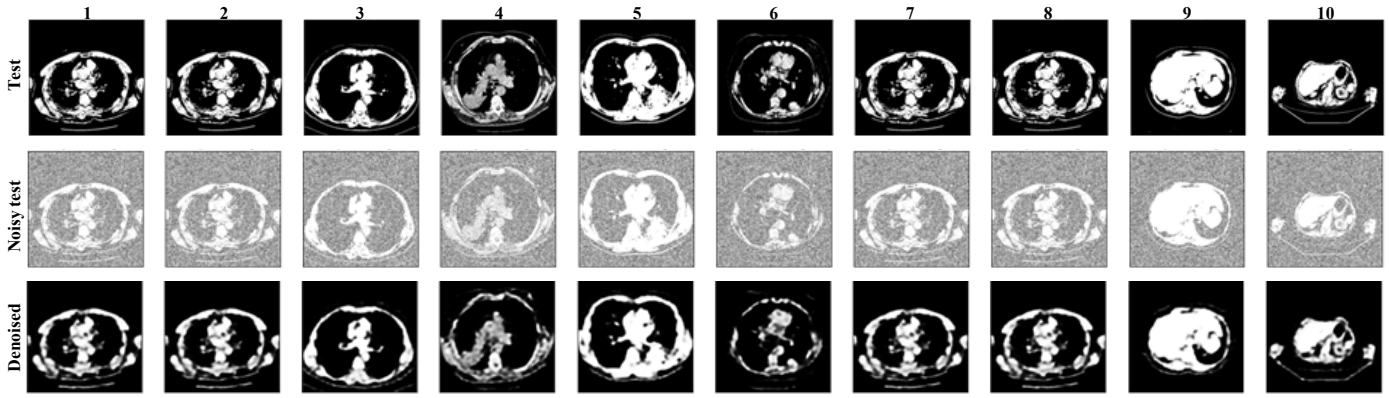

Figure 5. Visual comparison of random test images, noisy test images and denoised reconstructed images.

4. Conclusions

The study has proven to be a significant stride toward enhancing the quality of CT image reconstruction and denoising. Through the utilization of a deep autoencoder model, the study showcased promising outcomes, aiming to improve the accuracy of CT image reconstruction while mitigating noise interference. Several measures were used to assess the model's performance, including as Accuracy, Training and Validation Loss, and the Structural Similarity Index Measure (SSIM).

Throughout the testing and inference phases, the model consistently displayed an accurate reconstruction and denoising of CT images. The average SSIM score of 0.7613 between the test images and their Denoised Reconstructed counterparts indicates a moderate to good level of similarity in structural information, underpinning the model's ability to preserve crucial details during the denoising process. The SSIM measure highlights the model's ability to generalize its learning to new, unknown CT images while successfully decreasing noise interference when combined with the previously mentioned Training and Validation Loss metrics.

The study's findings demonstrate the model's excellent performance in denoising CT images, providing a basis for prospective future developments in medical imaging. But the study also identifies areas that need more investigation and development, especially when it comes to instances in which improving structural information preservation is necessary.

The importance of several measures in assessing the model's success is highlighted by this study. Remarkably, the model's accuracy during training reached 85.63% with a loss of 0.1278, and during validation, it scored 88.02% with a loss of 0.1052. The range of the SSIM spanned from 0.5721 to 0.8496, with an average score of 0.7613 across the entire test dataset. These metrics collectively portray the model's efficacy in denoising CT images, emphasizing its potential in the field of medical imaging.

References

[1] Webb A. Introduction to biomedical imaging. 2nd ed. New York: John Wiley & Sons Incorporated; 2022. 384 p.

[2] Gravel P, Beaudoin G, DeGuise JA. A method for modeling noise in medical images. IEEE Trans Med Imaging [Internet]. 2004 Oct;23(10):1221-32. Available from: https://doi.org/10.1109/tmi.2004.832656

[3] Kumar N, Nachamai M. Noise removal and filtering techniques used in medical images. Orient J Comput Sci Technol [Internet]. 2017 Mar 3;10(1):103-13. Available from: https://doi.org/10.13005/ojcst/10.01.14

[4] Chang Y, Yan L, Chen M, Fang H, Zhong S. Two-stage convolutional neural network for medical noise removal via image decomposition. IEEE Trans Instrum Meas [Internet]. 2020 Jun;69(6):2707-21. Available from: https://doi.org/10.1109/tim.2019.2925881

[5] Khan SU, Ullah N, Ahmed I, Ahmad I, Mahsud MI. MRI imaging, comparison of MRI with other modalities, noise in MRI images and machine learning techniques for noise removal: a review. Curr Med Imaging Former Curr Med Imaging Rev [Internet]. 2019 Feb 25;15(3):243-54. Available from: https://doi.org/10.2174/1573405614666180726124952

[6] Thanh D, Surya P, Hieu LM. A review on CT and X-ray images denoising methods. Informatica [Internet]. 2019 Jun 15;43(2). Available from: https://doi.org/10.31449/inf.v43i2.2179

[7] Tian C, Fei L, Zheng W, Xu Y, Zuo W, Lin CW. Deep learning on image denoising: an overview. Neural Netw [Internet]. 2020 Nov;131:251-75. Available from: https://doi.org/10.1016/j.neunet.2020.07.025

[8] Kadhim MA. Restoration medical images from speckle noise using multifilters. In: 2021 7th international conference on advanced computing and communication systems (ICACCS) [Internet]; 2021 Mar 19-20; Coimbatore, India. [place unknown]: IEEE; 2021. Available from: https://doi.org/10.1109/icaccs51430.2021.9441814

[9] Yadav SS, Jadhav SM. Deep convolutional neural network based medical image classification for disease diagnosis. J Big Data [Internet]. 2019 Dec;6(1). Available from: https://doi.org/10.1186/s40537-019-0276-2

[10] Elavaar Kuzhali S, Suresh DS. Advances in intelligent systems and computing [Internet]. Cham: Springer International Publishing; 2018. Patch-Based denoising with k-nearest neighbor and SVD for microarray images; p. 132-47. Available from: https://doi.org/10.1007/978-3-319-91186-1_15

[11] Heena A, Biradar N, Maroof NM, Bhatia S, Agarwal R, Prasad K. Machine learning based biomedical image processing for echocardiographic images. Multimedia Tools Appl [Internet]. 2022 Jul 27. Available from: https://doi.org/10.1007/s11042-022-13516-5

[12] Saleh Ahmed A, El-Behaidy WH, Youssif AA. Medical image denoising system based on stacked convolutional autoencoder for enhancing 2-dimensional gel electrophoresis noise reduction. Biomed Signal Process Control [Internet]. 2021 Aug;69:102842. Available from: https://

doi.org/10.1016/j.bspc.2021.102842
[13] Kumar VS, Jayalakshmi V. Reconstructing the medical image by autoencoder with stochastic processing in neural network. In: 2021 third international conference on inventive research in computing applications (ICIRCA) [Internet]; 2021 Sep 2-4; Coimbatore, India. [place unknown]: IEEE; 2021. Available from: https://doi.org/10.1109/icirca51532.2021.9545041
[14] Weng L. Lil'Log [Internet]. From Autoencoder to Beta-VAE; 2018 Aug 12. Available from: https://lilianweng.github.io/posts/2018-08-12-vae/.
[15] El-Shafai W, Abd El-Nabi S, M El-Rabaie ES, M Ali A, F Soliman N, D Algarni A, E Abd El-Samie F. Efficient deep -learning-based autoencoder denoising approach for medical image diagnosis. Comput Mater Amp Contin [Internet]. 2022;70(3):6107-25. Available from: https://doi.org/10.32604/cmc.2022.020698
[16] Laves MH, Ihler S, Kahrs LA, Ortmaier T. Semantic denoising autoencoders for retinal optical coherence tomography. In: Boppart SA, Wojtkowski M, Oh WY, editors. Optical coherence imaging techniques and imaging in scattering media [Internet]; 2019 Jun 23-27; Munich, Germany. [place unknown]: SPIE; 2019. Available from: https://doi.org/10.1117/12.2526936
[17] Chiang HT, Hsieh YY, Fu SW, Hung KH, Tsao Y, Chien SY. Noise reduction in ECG signals using fully convolutional denoising autoencoders. IEEE Access [Internet]. 2019;7:60806-13. Available from: https://doi.org/10.1109/access.2019.2912036
[18] Ghosh SK, Biswas B, Ghosh A. Advances in intelligent systems and computing [Internet]. Singapore: Springer Singapore; 2019. Restoration of mammograms by using deep convolutional denoising auto-encoders; p. 435-47. Available from: https://doi.org/10.1007/978-981-13-8676-3_38
[19] Paullada A, Raji ID, Bender EM, Denton E, Hanna A. Data and its (dis)contents: a survey of dataset development and use in machine learning research. Patterns [Internet]. 2021 Nov;2(11):100336. Available from: https://doi.org/10.1016/j.patter.2021.100336
[20] Albertina B, Watson M, Holback C, Jarosz R, Kirk S, Lee Y, Lemmerman J. Radiology data from the cancer genome atlas lung adenocarcinoma [tcga-luad] collection. The Cancer Imaging Archive. 2016;10:K9.
[21] Clark K, Vendt B, Smith K, Freymann J, Kirby J, Koppel P, Moore S, Phillips S, Maffitt D, Pringle M, Tarbox L, Prior F. The cancer imaging archive (TCIA): maintaining and operating a public information repository. J Digit Imaging [Internet]. 2013 Jul 25;26(6):1045-57. Available from: https://doi.org/10.1007/s10278-013-9622-7
[22] Mohd Sagheer SV, George SN. A review on medical image denoising algorithms. Biomed Signal Process Control [Internet]. 2020 Aug;61:102036. Available from: https://doi.org/10.1016/j.bspc.2020.102036
[23] Chollet F. Keras: Deep Learning for humans [Internet]. Keras: deep learning for humans; 2015 Mar 27. Available from: https://keras.io
[24] Wang Z, Bovik AC, Sheikh HR, Simoncelli EP. Image quality assessment: from error visibility to structural similarity. IEEE Trans Image Process [Internet]. 2004 Apr;13(4):600-12. Available from: https://doi.org/10.1109/tip.2003.819861
[25] Qiu Y, Yang Y, Lin Z, Chen P, Luo Y, Huang W. Improved denoising autoencoder for maritime image denoising and semantic segmentation of USV. China Commun [Internet]. 2020 Mar;17(3):46-57. Available from: https://doi.org/10.23919/jcc.2020.03.005

Acknowledgment

The authors would like to thank and acknowledge their work and academic colleagues, as well as the Digital Transformation Center (DTC) of Batangas State University, for their unwavering support and contributions to this study.